Distribution of seismic speed changes associated with the 12 May 2008 Mw 7.9 Wenchuan earthquake

Jiu Hui Chen,[1] Bérénice Froment,[2] Qi Yuan Liu,[1] Michel Campillo,[2]

We used continuous recordings in Sichuan, China to track the temporal change in elastic properties of the medium, namely the seismic speed, at a regional scale in a 2 year period which includes the great Wenchuan Mw 7.9 earthquake. The data are recorded by a temporary network of 156 broad-band seismographs, in a $200km \times 200km$ region that covers the southern 2/3 of the fault system activated during the Wenchuan event. Seismic noise cross correlation functions are computed in a 30-day moving window for periods between 1 and 3 seconds, and a doublet analysis is performed to detect temporal velocity changes with respect to a reference correlation. We found clear evidence that the seismic velocity drops by up to 0.08% in the fault region just after the earthquake while the measured velocity fluctuates within 0.02% before the earthquake. The co-seismic variation is therefore well above the resolution of the measurements. We compared the measurements in different subarrays to get a spatial distribution of the velocity change. This distribution is consistent with the stress change during the Wenchuan earthquake, as inferred from a kinematic model. We did not find that the co-seismic velocity variation is significantly larger for station groups in the Sichuan basin than in the Longmen Shan range, indicating that the co-seismic change is not controlled by the response of the sediments. On average the sensitivity to stress of the relative velocity change is of the order of $0.5 \times 10^{-8} Pa^{-1}$.

1. Introduction

On 12 May 2008, a Mw 7.9 earthquake struck Wenchuan, Beichuan and Qingchuan counties, China along the eastern margin of the Tibetan Plateau [*Burchfiel et al.*, 2008; *Zhang et al.*, 2008]. Surface geology surveys indicate a 240 km long rupture zone [*Xu et al.*, 2009]. Seismological data indicate that the rupture initiated in the southern Longmen Shan (LMS) (Figure 1) and propagated unilaterally northeastward on a northwest dipping fault for more than 320 km [*Ji and Hayes*, 2008]. Aftershock relocation results [*Chen et al.*, 2009] show that the dipping angle of the fault zone is $70^\circ \sim 80^\circ$ near the surface and is $30^\circ \sim 60^\circ$ near the hypocenter (14∼19 km depth).

Physical processes that accompany earthquakes, such as co-seismic stress changes, the migration of fluids and the formation of damage zones in the shallow layers, can cause changes in mechanical properties of nearby crustal material. Recently, technical and methodological developments have shown that such changes in material properties can be detected. Among them, ambient noise monitoring approaches [e.g. *Wegler and Sens-Schönfelder*, 2007; *Brenguier et al.*, 2008a, b], which use the coda of the noise correlation functions (NCFs), are specifically designed for continuous monitoring of temporal change in elastic properties of the medium (seismic speed), without repeating earthquakes or active sources. These studies are all relying on the extraction of the Earth response between two points from the correlation of seismic noise records [*Shapiro and Campillo*, 2004]. The nature of the later part of the NCF was analyzed by *Stehly et al.* [2008] who demonstrated that it contains at least partially the coda of the Green function. It was verified experimentally with ultra-sound that the coda of the NCF can be used for monitoring the velocity changes [*Hadziioannou et al.*, 2009]. The analysis of the correlation codas is based on the doublet method proposed for earthquake records [*Poupinet et al.*, 1984].

In October, 2006, that is, well before the Mw 7.9 Wenchuan earthquake, Institute of Geology of the China Earthquake Administration deployed almost 300 broadband stations in western Sichuan province, covering 2/3 of the fault system activated during the Wenchuan earthquake. This Western Sichuan Seismic Array (WSSA) was operational for more than 2 years and provides unique continuous recordings before, during and after the Wenchuan quake. The data obtained from WSSA were used to perform a series of studies related to the genesis and process of the Wenchuan earthquake, and the structure of the Eastern Tibetan Plateau [e.g. *Liu et al.*, 2009]. We use this data to investigate the change of crustal seismic velocity associated with the Wenchuan earthquake at the regional scale.

2. Data and measurement of relative velocity changes

Our study area comprises the northern part of the WSSA (29° to $32^\circ N$ and 100° to $105^\circ E$). We use 156 stations, with average station spacing of 20∼30 km. Figure 1 shows the location of the stations and the main geological units in this area. The stations are distributed in the LMS, the Sichuan Basin (SB), the Songpan-Ganzi (SG) and Chuan-Dian (CD) blocks. The closest station is within 20 km of the epicenter of the Wenchuan earthquake.

Data from January 1, 2007 to the end of 2008 are used in this study. Some stations near the epicenter of the Wenchuan May 12, 2008 earthquake suffered power failure during the main shock. These stations were recovered after at most 15 days. For the stations in operation in the days following the event, it was verified on-site that they were functioning correctly. This dataset has long enough recordings before and after the earthquake to allow for the study of the crustal velocity changes. The following paragraphs present the different steps of the processing applied to measure the temporal seismic velocity changes.

[1]State Key Laboratory of Earthquake Dynamics, Institute of Geology, China Earthquake Administration, Beijing 100029, China

[2]Laboratoire de Geophysique Interne et de Tectonophysique, CNRS & Univ. Joseph Fourier, Grenoble, France

0094-8276/10/$5.00

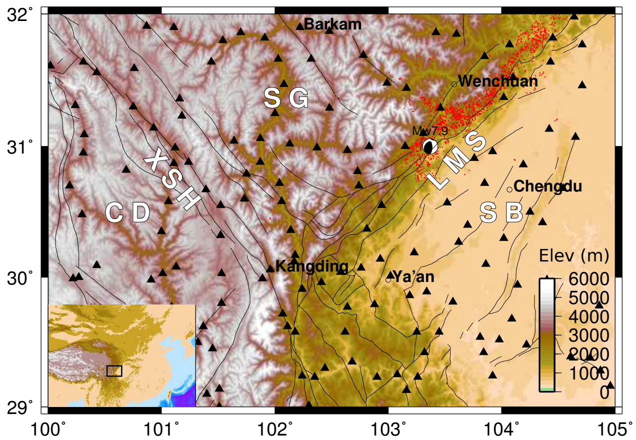

Figure 1. Stations used in this study (bold triangles) Black beach ball indicates the epicenter of the Wenchuan earthquake and red dots are aftershocks. Black lines are major faults in the studying region. SB, SG, CD, LMS and XSH stands for Sichuan basin, Songpan-Ganzi block, Chuan-Dian block, Longmen Shan fault zone and Xianshuihe fault zone respectively.

We first resample the data to 5 sps. A time domain normalization method is used to remove effects of strong localized energetic signal principally due to earthquakes and locally generated noise. The data preprocessing is the same as in *Yao et al.* [2006]. We consider every possible station pairs with a spacing less than 200 km. We compute the NCFs of 30-day moving windows for periods between 1 and 3 seconds. We interpret the NCFs as an approximation of the actual Green function between the stations. The window duration of 30 days was chosen after testing the stability of the NCF versus window lengths. Figure 3 shows an example of the NCFs varying with time. It shows that the NCFs are well defined throughout the 2-year period. The direct wave amplitude shows seasonal variations that reflect changes in noise excitation. The coda waves show arrivals that remain

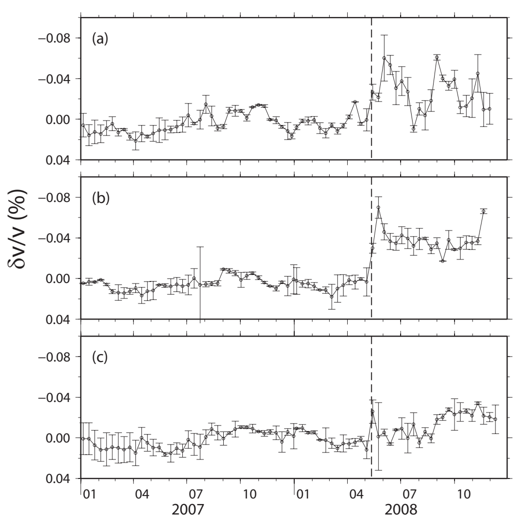

Figure 2. Relative temporal velocity changes for (a) the Sichuan Basin (b) the Longmen Shan fault belt, and (c) the Songpan-Ganzi block. The vertical dashed line indicates the date of the Wenchuan Mw7.9 earthquake

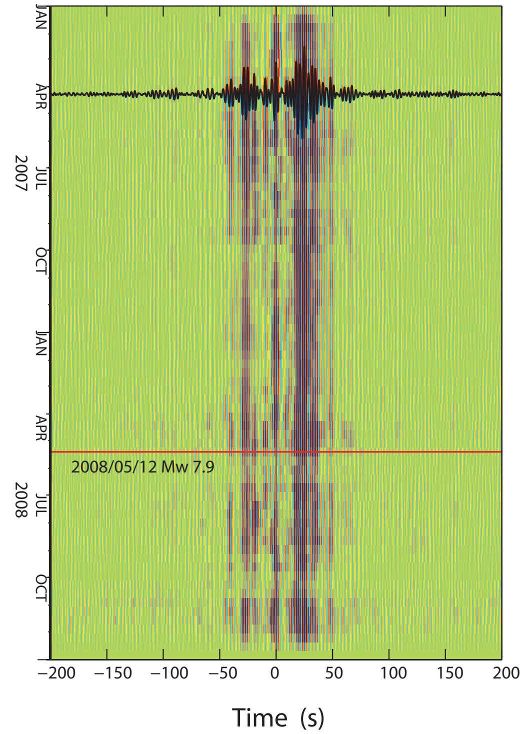

Figure 3. 30-day stacked NCF for the station pair KWC05 and KCD01. The amplitude of the NCFs are in arbitrary unit. The distance between the 2 stations is 60.2 km. The thick black curve represents the reference stacked NCF. The red line indicates the date of the Wenchuan earthquake.

stable over the whole 2-year period. In order to attenuate the effects of temporal variations in the distribution of the noise sources, we ignored the direct waves which are highly sensitive to azimuthal distribution of the noise intensity [e.g. *Froment et al.*, 2010]. We thus consider a window that starts long after the ballistic arrivals, which is about 25 s in Figure 2. We investigate travel time variations between NCFs using the coda of up to ± 200 s lapse time. While calculating the NCFs, instrumental timing errors are checked by both the State-of-Health record of the instrument and by checking the time symmetry of the noise correlations [*Stehly et al.*, 2007]. Stations exhibiting instrumental timing problems have been removed.

For each station pair, the NCFs stacked over the 2-year period of study defines the long-term reference trace. Travel time variation with respect to the reference trace is calculated for each 30-day NCF with the doublet method. For a specific region and date, delays δt at lapse time τ for all the station pairs are averaged, and a linear least-square regression is applied to get the relative travel time change ($\delta t/\tau$) for the specific date and region of interest. The relative velocity change is the opposite of the travel time change rate ($\delta v/v = -\delta t/\tau$).

3. Results

3.1. Temporal velocity changes

The measurements of the velocity changes for the groups of stations in the LMS fault belt, SG and SB blocks are shown in Figure 2. We note relatively weak velocity variation before the Wenchuan earthquake, sharp co-seismic velocity changes in LMS and SB, and restoring after the earthquake. A long-term relaxation cannot be analyzed with the available records.

The velocity fluctuation before the Wenchuan earthquake for the 3 regions is within $\pm 0.02\%$. This is similar to what was observed before the Parkfield earthquake by *Brenguier et al.* [2008b].

The temporal variations are different in the three regions (Figure 2). The seismic velocity drop reached a value about 0.08% just after the Wenchuan earthquake in the region close to the LMS fault. This is a bit larger, but of the same order as found for the M6.0 Parkfield earthquake [*Brenguier et al.*, 2008b]. Note that the network in Parkfield was just at the epicentral region with a spatial extension of about 20 km, which was of the order of the rupture size of the earthquake; WSSA has an aperture of about 300 km, which is also the length of the Wenchuan rupture. The similarity of the average change of velocity is probably an expression of the earthquake scaling law with almost constant stress drop.

3.2. Spatial distribution of the co-seismic velocity changes

The dense and nearly even spatial station distribution of the WSSA makes it possible to investigate the spatial distribution of velocity changes over the full region. To do this, we define a grid of $0.5^\circ \times 0.5^\circ$ sub-regions. The stations considered for each small region are within 0.5° from the center of the region (see Figure A in auxiliary material). Note that we produce a smoothed regionalization, in agreement with the fact that we use coda waves with average lapse time of about 100 s that sample a wide zone. The co-seismic velocity change obtained for each of the sub-region is estimated as the difference between the velocities which were averaged over the period before the earthquake and over the 50-days after. Figure 4 shows the spatial distribution of the estimated co-seismic velocity changes. Since the fluctuation of the measured velocity before the earthquake is $\pm 0.02\%$, only regions where the co-seismic velocity change is larger than 0.02% are considered to have been affected by the earthquake.

The velocity clearly dropped in a wide zone around the LMS, where the aftershocks are distributed. On the contrary, the crustal velocity hardly changed in the southern part of the LMS. Figure 4 shows that the velocity drop in SB is similar as that in the SG block. We evaluate the consistency of the velocity drop with the elastic static stress change associated with the earthquake. We consider the normal stress for a fault with the orientation of the main rupture. The stress change is deduced from the kinematic model of [*Ji and Hayes*, 2008; *Parsons et al.*, 2008, Shao and Ji, 2009 pers. comm.]. (See auxiliary material Figure B.).

The map of velocity change has clear similarities with the static stress changes, which suggests that the two are causally related. We notice on Figure 4 a small region of velocity drop centered in $29.5^\circ N, 102.5^\circ E$. This is also the place of an anomaly in the intensity map [*Li et al.*, 2008]. A zone of destructions with intensity VIII was reported in this area, suggesting a strong local site amplification, likely related with the response of shallow soft materials, superficial layers would have been severely affected by the shaking, resulting in a local drop of velocity. Nevertheless, at the regional scale, the velocity drop exhibits a better correlation with the static stress change than with the surface geology or the intensity map.

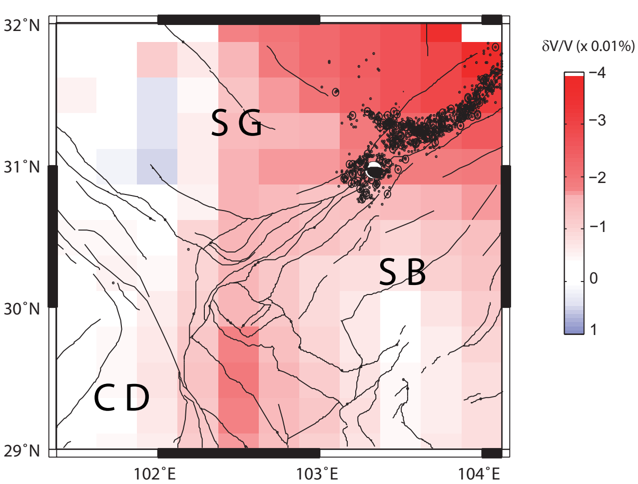

Figure 4. Distribution of co-seismic relative velocity changes. The beach ball indicates the epicenter of the Wenchuan earthquake, bold circles and small dots are aftershocks, thick lines are major faults in the region.

4. Discussions and Conclusions

This study demonstrates that, despite less rigorous station installation for this temporary network than for the permanent borehole stations of HRSN network in Parkfield, temporal velocity monitoring can be achieved with a similar resolution. We also show that the velocity change is detectable at the regional scale.

Our results found a maximum of 0.08% velocity drop just after the Wenchuan Mw 7.9 earthquake. The relative velocity change is only slightly larger than that of the 2004 Parkfield Mw 6.0 earthquake [*Brenguier et al.*, 2008b], which shows that the velocity changes during an earthquake is not increasing with the total moment released. This results from the almost constant stress drop observed during earthquakes of various Mw. The velocity changes are found not only in the regions with sedimentary covers but also in the high plateau, showing that damage in the sedimentary cover is not the only cause of the temporal variations. The spatial distribution of the co-seismic velocity changes is consistent with the distribution of normal stress changes associated with the main shock.

In this study we consider coda waves propagating, on average, for 100 s. For the region close to the LMS fault, these waves sample medium within a 150-km-radius zone around the fault. We evaluate the average normal stress change in the region from the static elastic stress change produced by the rupture obtained by [*Ji and Hayes*, 2008] (Figure B in the auxiliary material). The average stress change is about $10^5 Pa$. We thus infer a sensitivity of relative velocity change to stress on the order of $0.5 \times 10^{-8} Pa^{-1}$. This value should be compared to the direct measurement of *Niu et al.* [2008] at a depth of 1 km at SAFOD, that is $2.4 \times 10^{-7} Pa^{-1}$. Our observation is more than one order of magnitude smaller. This difference can be attributed to the fact that our measurements are sensitive to larger depths, where material can be expected to be less weathered or cracked, than the data used in the San Andreas fault study.

Acknowledgments. The study was jointly supported by the Key Projects of Chinese National Programs for Fundamental Research and Development (2004CB418402), the National Natural Science Foundation of China (40974023) and the European Research Council (Advanced Grant Whisper). B.F. acknowledges financial support from Shell Research. Guangfu Shao and Chen Ji kindly provided results of their stress changes. Shuncheng Li, Biao Guo, Yu Li, Jun Wang and Shaohua Qi participated to the acquisition of field data. We thank Florent Brenguier, Céline Hadziioannou, Philippe Roux, Nikolai Shapiro, Huajian Yao and Rob van der Hilst for helpful discussions.

References

Brenguier, F., N. M. Shapiro, M. Campillo, V. Ferrazzini, Z. Duputel, O. Coutant, and A. Nercessian (2008a), Towards forecasting volcanic eruptions using seismic noise, *Nature Geoscience*, *1*, doi:10.1038/ngeo104.

Brenguier, F., M. Campillo, C. Hadziioannou, N. M. Shapiro, R. M. Nadeau, and E. Larose (2008b), Postseismic relaxation along the San Andreas Fault at Parkfield from continuous seismological observations, *Science*, *321*, 1478–1481, doi: 10.1126/science.1160943.

Burchfiel, B. C., L. H. Royden, R. D. van der Hilst, Z. Chen, R. W. King, C. Li, J. Lü, and H. Yao (2008), A geological and geophysical context for the Wenchuan earthquake of 12 may 2008, Sichuan, People's Republic of China, *GSA Today*, *18*(7), doi:10.1130/GSATG18A.1.

Chen, J. H., Q. Y. Liu, S. C. Li, B. Guo, Y. Li, J. Wang, and S. H. Qi (2009), Seismotectonic study by relocation of the Wenchuan ms 8.0 earthquake sequence, *Chinese J. Geophys.*, *52*(2), 390–397, in Chinese.

Froment, B., M. Campillo, P. Roux, P. Gouédard, A. Verdel, and R. Weaver (2010), Estimation of the effect of non-isotropically distributed energy on the apparent arrival time in correlations, *Geophysics*, in press.

Hadziioannou, C., E. Larose, O. Coutant, P. Roux, and M. Campillo (2009), Stability of monitoring weak changes in multiply scattering media with ambient noise correlation: Laboratory experiments, *J. Acoust. Soc. Am.*, *125*(6), doi: 10.1121/1.3125345.

Ji, C., and G. Hayes (2008), Preliminary result of the May 12, 2008 Mw 7.9 eastern Sichuan, China earthquake, *US Geol. Surv.*, http://earthquake.usgs.gov/eqcenter/ eqinthenews/2008/us2008ryan/finite_fault.php.

Li, Z., Y. Yuan, X. Li, Q. Zhang, Q. Zhang, B. Y. Dai, Y. Q. Ye, P. F. Ge, and J. Zheng (2008), Preliminary research on the characteristics of the Ms8.0 Wenchuan earthquake hazard, *Seismology and Geology*, *30*(4), 855–876.

Liu, Q. Y., Y. Li, J. H. Chen, and et al. (2009), Wenchuan ms 8.0 earthquake: preliminary study of the S-wave velocity structure of the crust and upper mantle, *Chinese J. Geophys.*, *52*(2), 309–319, in Chinese.

Niu, F., P. G. Silver, T. M. Daley, X. Cheng, and E. L. Majer (2008), Preseismic velocity changes observed from active source monitoring at the Parkfield SAFOD drill site, *Nature*, *454*, 204–208, doi:10.1038/nature07111.

Parsons, T., C. Ji, and E. Kirby (2008), Stress changes from the 2008 Wenchuan earthquake and increased hazard in the Sichuan basin, *Nature*, *454*, 509–510, doi: 10.1038/nature07177.

Poupinet, G., W. L. Ellsworth, and J. Frechet (1984), Monitoring velocity variations in the crust using earthquake doublets: an application to the Calaveras Fault, California, *J. Geophys. Res.*, *89*, 57195731.

Shapiro, N. M., and M. Campillo (2004), Emergence of broadband Rayleigh waves from correlations of the ambient seismic noise, *Geophys. Res. Lett.*, *31*, L07,614, doi:10.1029/2004GL019491.

Stehly, L., M. Campillo, and N. M. Shapiro (2007), Traveltime measurements from noise correlations: stability and detection of instrumental time-shifts, *Geophys. J. Int.*, *171*, 223–230, doi:10.1111/j.1365-246X.2007.03492.x.

Stehly, L., M. Campillo, B. Froment, and R. L. Weaver (2008), Reconstructing Green's function by correlation of the coda of the correlation (C^3) of ambient seismic noise, *J. Geophys. Res.,* , *113*, B11,306, doi:10.1029/2008JB005693.

Wegler, U., and C. Sens-Schönfelder (2007), Fault zone monitoring with passive image interferometry, *Geophys. J. Int.*, *168*, 1029–1033, doi:10.1111/j.1365-246X.2006.03284.x.

Xu, X. W., X. Z. Wen, G. H. Yu, G. H. Chen, Y. Klinger, J. Hubbard, and J. Shaw (2009), Coseismic reverse- and oblique-slip surface faulting generated by the 2008 mw 7.9 Wenchuan earthquake, China, *Geology*, *37*(6), 515–518, doi: 10.1130/G25462A.1.

Yao, H. J., R. D. van der Hilst, and M. V. de Hoop (2006), Surfave-wave array tomography in SE Tibet from ambient seismic noise and two-station analysis - I. phase velocity maps, *Geophys. J. Int.*, *166*, 732–744.

Zhang, P. Z., X. W. Xu, X. Z. Wen, and et al. (2008), Slip rates and recurrence intervals of the Longmen Shan active fault zone, and tectonic implications for the mechanism of the May 12 Wenchuan earthquake, 2008, Sichuan, China, *Chinese J. Geophys.*, *51*(4), 1066–1073, in Chinese.

Jiu-Hui Chen and Qi-Yuan Liu, State Key Laboratory of Earthquake Dynamics, Institute of Geology, CEA, Beijing 100029, China

Bérénice Froment and Michel Campillo, Laboratoire de Geophysique Interne et de Tectonophysique, CNRS & Univ. Joseph Fourier, Grenoble, France